Prepared for submission to JINST

8th International Symposium on Negative Ions, Beams and Sources
October 2 - 7, 2022
Orto Botanico - Padova, Italy

Comparison among possible design solutions for the Stray Field Shielding System of the DTT Neutral Beam Injector

Fabio Veronese,[a,b,1] **Piero Agostinetti,**[a,c] **Giuseppe Calabrò,**[d] **Flavio Crisanti,**[d] **Pierluigi Fanelli,**[d] **Riccardo Lombroni,**[d] **and Andrea Murari**[a,c]

[a] *Consorzio RFX (CNR, ENEA, INFN, University of Padova, Acciaierie Venete S.p.A.), Corso Stati Uniti 4, Padova, 35127, Italy*
[b] *Centro Ricerche Fusione (CRF), Università di Padova, Corso Stati Uniti, 4, Padova, 35127, Italy*
[c] *Institute for Plasma Science and Technology - Section of Padova, Corso Stati Uniti 4, Padova, 35127, Italy*
[d] *DEIM, Università degli Studi della Tuscia, Largo dell'Università, Viterbo, 01100, Italy*

E-mail: fabio.veronese@igi.cnr.it

Abstract: Within the effort on the conceptual design of the Divertor Test Tokamak (DTT) Neutral Beam Injector (NBI), the design of the Stray Field Shielding System (SFSS) for DTT NBI is under development, to suppress the potentially harmful effects of the stray poloidal field from the tokamak on the accelerated charged beam. Various possible design solutions to solve this problem are presented and compared, with a particular focus on the stray field minimization procedure and particle tracing simulations, used during the design validation phase with the objective of maximizing beamline performances.

Keywords: Accelerator modelling and simulations, Accelerator Subsystems and Technologies

[1] Corresponding author.

Contents

1 Introduction

The main purpose of the Divertor Tokamak Test facility is to study alternative solutions to mitigate the issue of power exhaust under integrated physics and technical conditions relevant for ITER and DEMO [1]. The proposed device features a Neutral Beam Injector heating system, providing deuterium neutrals (D^0) with an energy of 510 keV and an injected power of 10 MW to the tokamak chamber (Figure 1). A tokamak magnetic system is by definition composed by a main toroidal coil system providing the principal confinement for the plasma, and a poloidal (vertical and radial) coil system dedicated to provide flux swing, vertical stability, shape control, etc. The toroidal coil system aims to approximate a perfect toroidal configuration, but by obviously having only discrete sets of coils, part of the field "leaks" through the gaps, creating the so-called ripple field which causes additional plasma losses; this field however decays quickly with increasing radial distance, so it is not a problem for far enough devices. However, this is different for the poloidal system, whose solenoidal structure allows for free expansion of the magnetic dipole field around the tokamak, with the field decaying slowly. This field is referred to as the *poloidal stray field* (Figure 2). Due to the nature of their operation related to fast, charged particle beams, NBIs are particularly susceptible to external electromagnetic fields; when coupled to a large tokamak where high magnetic fields are a requirement, issues regarding charged beams are bound to arise. This is especially true for DTT, where the NBI is being positioned fairly close to the tokamak (within about 7 to 15 m from the magnetic axis), while being subjected to scenarios devised to be ITER and DEMO-like. Confirmation about the importance of this problem was obtained during the first particle tracing simulations, which made use of a full map of the tokamak's magnetic field to determine wall power losses on the Beam Line Components (BLCs): the field was confirmed strong enough to deflect 99 % of the beam upon the neutralizer; the remaining 1 % being the part of the beam that managed to neutralize before being deflected in the short space between the Grounded Grid (GG) and the

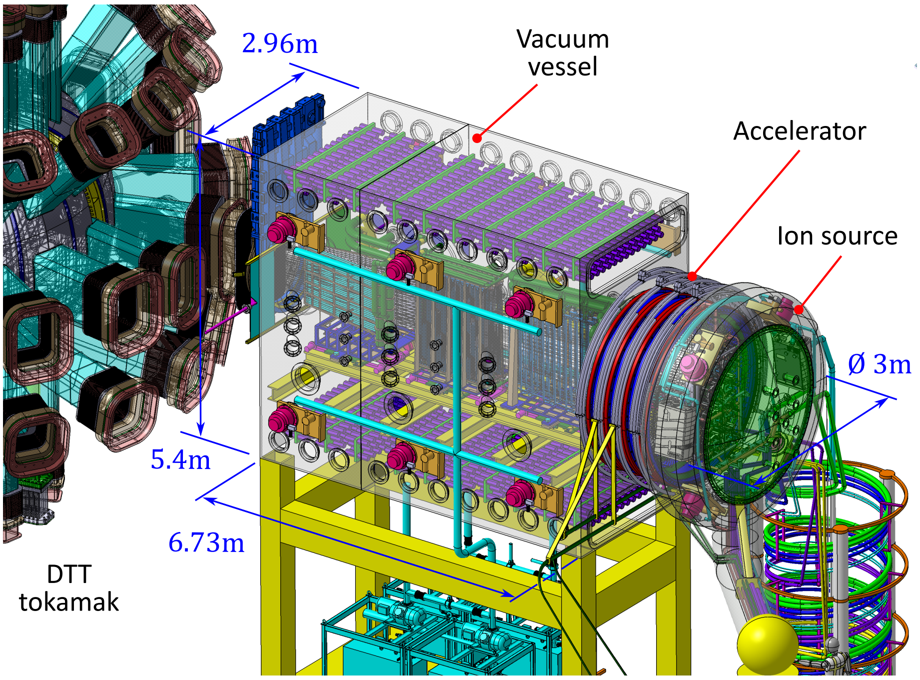

Figure 1. Overall view of DTT NBI in its position near the DTT tokamak; main dimensions of the vessel are also reported.

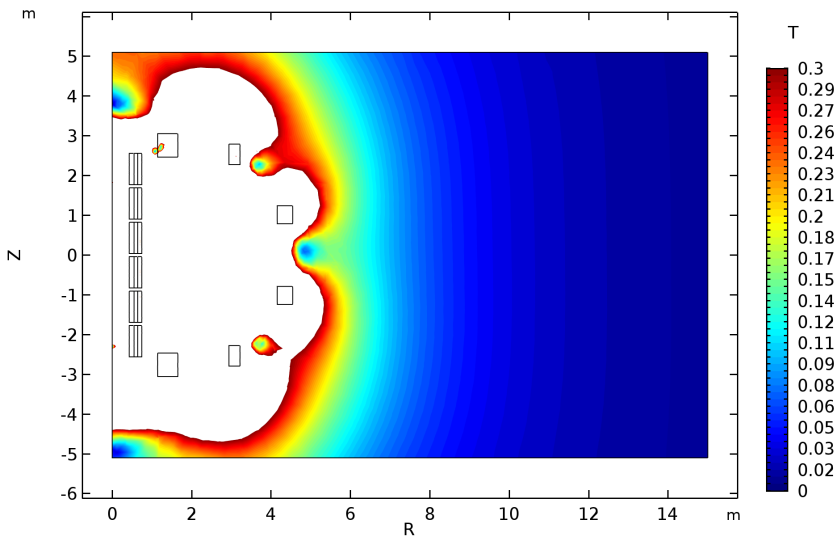

Figure 2. Contour plot for the absolute value of the magnetic flux density, showing the extension of the poloidal stray field. The value range is limited to appreciate the field in the farthest region.

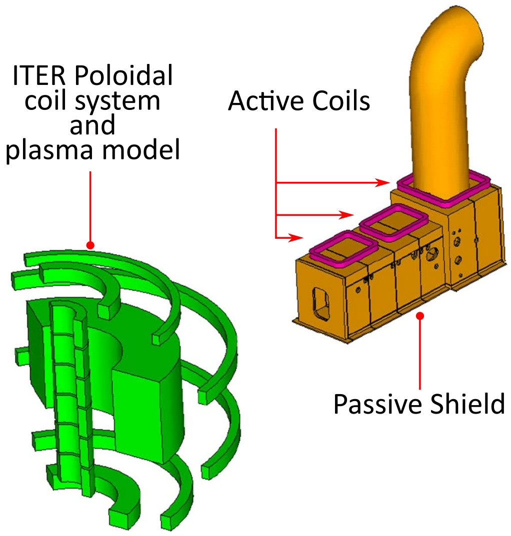

Figure 3. An older ITER MFRS design [5] as an example of a stray field compensation system.

neutralizer. This motivated a significant research programme to identify a method of suppressing the stray field effect.

2 Stray Field Shielding System

The correction for the stray field has been already implemented to various degrees in all existing operating tokamaks featuring NBI such as JT-60 [2] and ASDEX-UG [3], and ITER NBI itself is going to feature a large Magnetic Field Reduction System (MFRS) [4, 5]; the DTT version will be denominated Stray Field Shielding System (SFSS). All of the considered design solutions are based on one of the following systems, or both (illustrated in Figure 3):

- A ferromagnetic structure (Passive Shield, PS), dedicated to re-routing the field around the desired regions.
- If that is not enough, also an Active Coil (AC) system to suppress the constant "error" given by the passive shield and to follow the evolution of the stray field as it evolves in time during a discharge.

The region that these shields need to protect is usually the one where charged particles are present, meaning the beam source, the electrostatic accelerator, and the neutralizer, until the Residual Ion Dump (RID). For the scope of this paper, the region to shield has been restricted to the region downstream of the GG, since the beam source and the accelerator are complex components that require their own specific set of codes to evaluate external effects; these regions will be object of a separate work. The ideal placement of these components depends on each particular case:

- Outside the vacuum vessel, occupying more space and needing to enclose regions larger than needed, but with no drawbacks on the beam itself and easily accessible.

- Inside the vacuum vessel, minimizing the region to shield, but with potential issues due to the beam operation, e.g., obstruction of gas flow, voltage holding, coil feed-through, etc.

In the case of DTT NBI the space constraints, the air-insulated beam source requiring a large external clearance, and the possible adverse effects of having a large iron mass close to the tokamak fields, make the use of passive external shielding unattractive.
Efforts in designing the SFSS concentrated around this fact, producing a series of proposed designs which are the object of the paper:

- The first design is an external active coil system, which has been useful in determining the quantities at play needed to suppress the stray field; referred to as the "reference" case due to its status of first solution proposed.
- The second design is a fully passive internal shield, wrapping tightly around the interested region; it was proposed to analyse the possibility of avoiding coils entirely.
- The third design is the combination of the second design with additional active coils (located in this case inside the vacuum vessel), in order to increase the minimization of the stray field.

Each of the designs will be described in detail in the following paragraphs.

3 Problem setup

Before going into the detail of each design, the simulation procedure is described. First, the poloidal stray field must be obtained: to achieve this, a sector of the DTT tokamak (one sixth) containing the outline of DTT NBI has been modelled using the commercial multi-physics Finite Element Method (FEM) code COMSOL®.

The simulation is a linear magnetostatic problem, to shorten computational time and hence allowing for a quick adjusting of the geometry in-between runs. The material used in the passive structures is always the same iron model material, characterized by a constant relative permeability of $\mu_{Fe} = 4000$. While obviously not ideal, since real high permeability ferromagnetic materials are non-linear, at this early point of the investigation of the issue it is an unnecessary complication. Care was taken however in sizing appropriately the shield thickness and shape such that the resulting field may not be over the saturation point of a hypothetical ferromagnetic material, meaning around 0.8 to 0.9 T.

To limit the volume needed to properly simulate the tokamak without edge effects, the model is set up to have an cylindrical coordinate system ($\mathbf{i}_\phi$ for toroidal direction, $\mathbf{i}_r$ for radial, $\mathbf{i}_z$ for vertical), with symmetry conditions placed at the two lateral planes delimiting the simulation domain, while the upper, lower and outer side of the domain contain a special layer called *Infinite Element Domain*, wherein the mesh elements are artificially scaled up in length during calculation to emulate a very large domain for a fraction of the volume. An example domain is reported in Figure 4. To calculate the stray field, information is needed on the particular scenario that is being implemented, and since the coil currents vary considerably for the same scenario, also the time history of the plasma discharge must be considered. Given the preliminary nature of the work, it was decided to focus on the baseline Single Null (SN) DTT scenario, and to simplify the computational effort, only the time

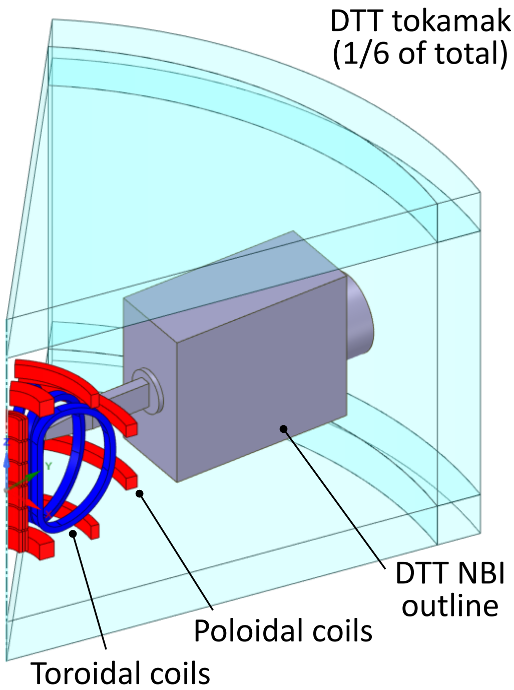

Figure 4. Simulation domain of the magnetostatic problem in COMSOL.

of maximum field within the NBI (found to be immediately after the phase of flat-top, at $t = 89$ s) was considered. During exploration of the stray field shape and strength, the vertical component B_z was found to be predominant within the NBI region, as a consequence of the NBI location along the equatorial plane ($z = 0$). Coupled with the fact that this component is the main responsible for the particle losses on the tall and thin walls of the Beam Line Components (BLCs) due to its sideways deflection, it is safe to restrict the scope of minimization to only the B_z component of the stray field.

Once established the boundary conditions of the tokamak, the type of SFSS to test must be chosen: if the design features a Passive Shield, its geometry is added to the model to determine the new resulting stray field distribution. The field within the whole NBI is not necessary at this step, so a small volume enclosing the space between the GG and the Neutralizer (where the charged beam will travel through) is individuated and denominated the *evaluation volume* V, which will be the target of shielding and field minimization. If the design features Active Coil(s), they are also added to the model; however, the procedure for choosing the correct set of coil currents needs to be considered. To do this, a separate simulation for each coil or coil pair imposing a test current of 1 A when all of the other sources are turned off is carried out, and the resulting field within the evaluation volume V is exported for each one. In linear conditions, this allows to directly scale up the coil fields with the imposed currents and add them to the stray field for each point within the volume V. This results in an overdetermined system of the type

$$\sum_{i}^{N_c} B_{c,i_z}(P) \cdot I_{c,i} + B_{s_z}(P) = 0, \;\; P \in V \tag{3.1}$$

where N_c is the total number of coils or coil pairs, $B_{c,i_z}(P)$ is the vertical field generated at point

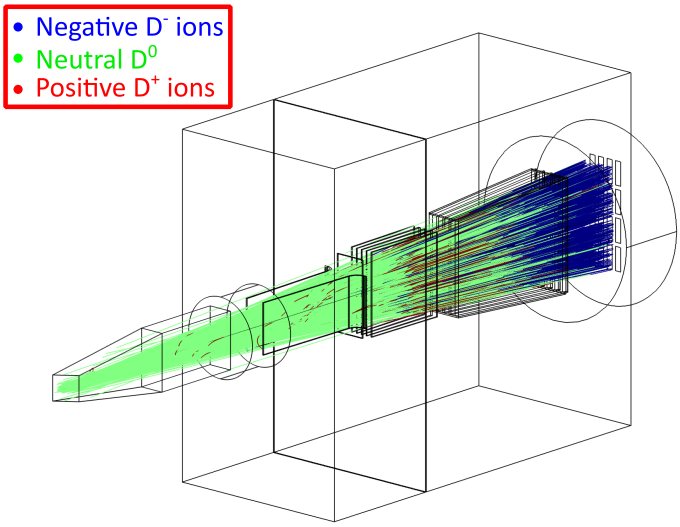

Figure 5. Result of a particle tracing simulation in COMSOL.

P per each ampere of current through the i-th coil, $I_{c,i}$ is the current flowing to the i-th coil and $B_{s_z}(P)$ is the vertical field generated at point P by the stray field. To minimize this system various optimization methods can be utilized; in this case, the fastest way to obtain a result is to simply look for the least squares solution to the system: the current vector $\mathbf{I_c}$ thus obtained can be used for one final simulation where all field sources are active, and the whole NBI field exported. In parallel, if the chosen SFSS has internal components, the neutral gas distribution may be affected, and needs to be recalculated to later estimate the correct beam evolution: COMSOL allows to simulate the vacuum system as well. The formulation used is a typical approach to vacuum system modelling, the isothermal angular coefficient method [6], which treats gas flow akin to radiation exchange: the code calculates the view factors between elements and models diffusion off of the walls between sources and sinks using a cosine law of reflection.

The last step is to combine the exported compensated field and gas distribution in a full-NBI particle tracing simulation, where it is possible to evaluate directly the efficacy of the chosen SFSS configuration by the most important quantity: the neutral power successfully transmitted to the plasma (Figure 5). This aspect is the basis of the main figure of merit used in this work, the *compensation efficiency* η_{stray}, defined as

$$\eta_{stray} = \frac{P_{pl}}{P_{pl,\,\text{no-field}}} \tag{3.2}$$

where P_{pl} is the neutral power reaching the exit of the NBI duct for a given setup, and $P_{pl,\,\text{no-field}}$ is the same quantity calculated in a completely stray field-free case: this number can be used as an additional factor within the efficiency tower to obtain the NBI wall-plug efficiency and is tied to each specific SFSS. If the value is satisfactory, then other quantities will come into consideration to decide if the design is viable such as current magnitude needed (if active), encumbrance, saturation, etc. The calculated value for $P_{pl,\,\text{no-field}}$ that will be used is 9.94 MW.

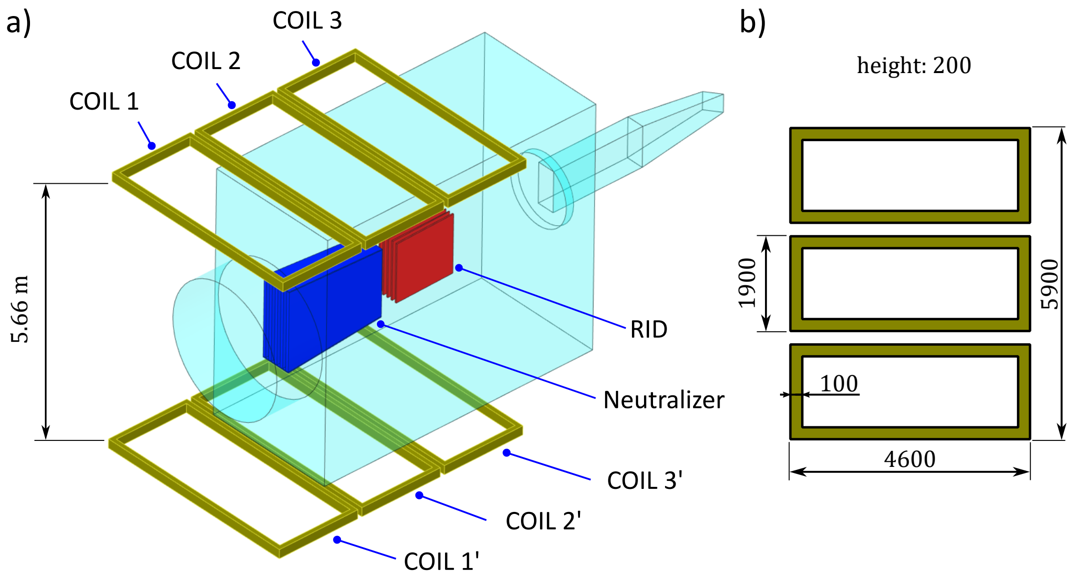

Figure 6. Case 1, a) View of the external coil system applied to DTT; b) detail of the coil dimensions (not to scale).

4 Comparison of the various SFSS designs

4.1 Case 1: external Active Coils

This design was the first functioning result that was found during the early design phase, when passive shields were still not being considered for simplicity, and the effort was aimed at finding a solution external to the NBI vacuum vessel: this would be quite desirable to avoid accessibility issues and to avoid disrupting the internal gas flow. The solution comprises 3 pairs of nested coils, placed side-to-side. The geometry is detailed in Figure 6. Each coil pair works in Helmholtz configuration (same current and orientation), and their particular geometry allows them to follow accurately the shape of the stray field. The design is fairly simple and not optimized in sizes and placement; the main guideline however is to place the coils in order to have the maximum effect on the early stage of the neutralization. This can be a problem, since in that region many high-voltage components are present, and the presence of additional coils may case issues with the voltage holding.

Another issue of this design is the large distance of the coils from the desired shielding region: this forces the design currents to be extremely high in order to reach the desired compensation effect, thus requiring specific power supplies, being difficult to control, or even causing disturbances to the tokamak field.

The optimized coil currents are reported in Table 1; the calculated compensation efficiency is an interesting $\eta_{stray} = 0.925$.

4.2 Case 2: internal Passive Shield

This design is the diametrically opposite approach to the previous: after noticing the issues with the external coils, the option of introducing passive shields was taken into consideration. When

Coil pair	Design currents [kAt]
Coil 1 - 1’	101
Coil 2 - 2’	77
Coil 3 - 3’	276

Table 1. Design currents of Case 1. The sign of the currents depends on the orientation of the external field.

deciding whether using a large, external shield or a smaller, internal one, the issue of field leakage within the shielding region became apparent: to put it simply, when a shield encloses a region but presents an aperture on its surface, the magnetic field will "leak" inside for a distance proportional to the smallest dimension of said aperture. For an external shield, this means that the whole vessel should be covered in iron, leaving only the duct aperture, or that at the very least the shield should overextend over the desired volume V to minimize for the leakage. Both of these options however would require a massive amount of iron near the DTT tokamak, which is not acceptable; internal shields were therefore considered. Apertures must still be present to allow beam passage, but leakage can be controlled by over-extension after the neutralizer, and application of a *Barrier Grid* (BG) on the GG (Figure 7). This BG will rest on the GG with apertures large enough to not affect the beam, serving as a "lid" to the rest of the shield in a very delicate zone that otherwise would be subjected to unmitigated field leakage.

As mentioned before, having an internal shield changes the background gas distribution; especially in this case, where the shield is wrapped tightly around the neutralizer, the flow to the pumps in the zone between GG and neutralizer is completely blocked, potentially causing issues of premature stripping inside the accelerator due to increased gas density. To mitigate this, an array of apertures is foreseen all around the shield, their radius chosen as to reduce leakage while allowing gas flow to a suitable degree. The result is an almost perfect insulation of the shielded region, and quite promising for a fully passive system (with compensation efficiency $\eta_{stray} = 0.961$). A quick scan of the diameters for apertures on the shield individuated a 100 mm diameter as sufficiently limiting field leak; on the sides, apertures are placed and offset as to maximize empty space while avoiding saturation. The apertures did help in decreasing the gas density outside the GG (to about 50 % higher value than the original case) but the gas flow from the neutralizer still had to be adjusted in order to have the ideal target thickness and maximize neutralization. A colour map of the magnetic flux density on the shield is reported in Figure 8.

4.3 Case 3: internal PS and AC system

The last design considered is an improvement upon the second case: the Passive Shield is the same, while adding a single Active Coil pair in Helmholtz configuration. Their geometry follows the shield in its inclination and is tailored to fit within the beam source aperture with no mechanical interference (Figure 9). The result of increased complexity is improved field minimization: $\eta_{stray} = 0.981$. The most important positive aspect is that now only one pair of coils is sufficient, and that the required current to minimize the worst-case field is 33 kAt, one order of magnitude less than the external coil design, due to them being closer now.

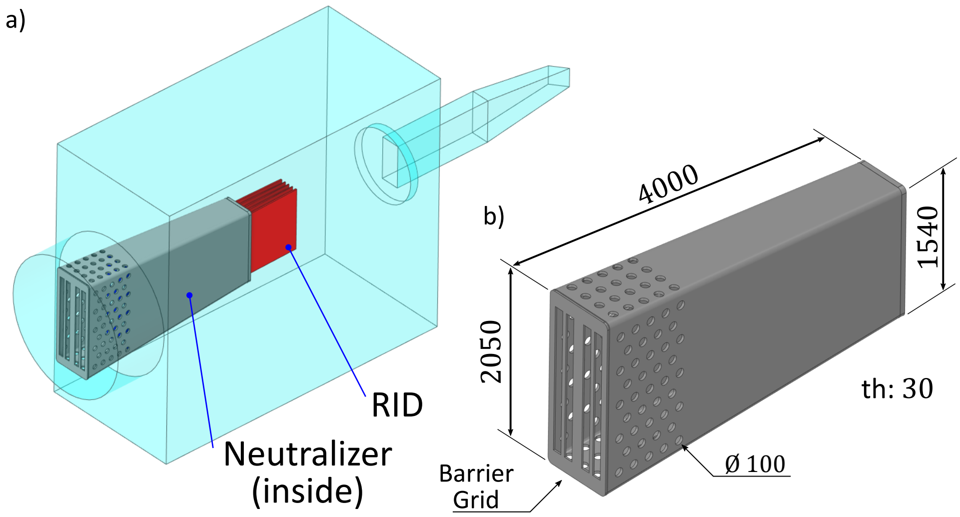

Figure 7. Case 2, a) View of the internal passive shield applied to DTT; b) detail of the shield.

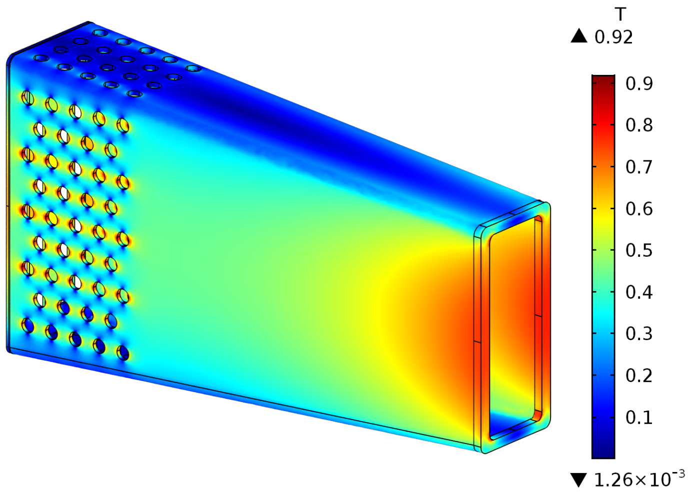

Figure 8. Colour map of the absolute value of the magnetic flux density on the Passive Shield. The region near the RID is subjected to a stronger field, reaching near to 0.92 T.

5 Conclusions

With this paper, a comparison between possible SFSS designs for DTT NBI has been carried out, highlighting first the priorities that a successful design should possess, and then verifying each one through an integrated suite of models that are able to cover multiple physics aspects at the same time. This allowed for each design to directly obtain a useful quantity, the compensation efficiency (with the results summarized in Table 2), which together with other dimensioning parameters, can be used to proceed with the design with a clear view on how to deal with the problem of the poloidal

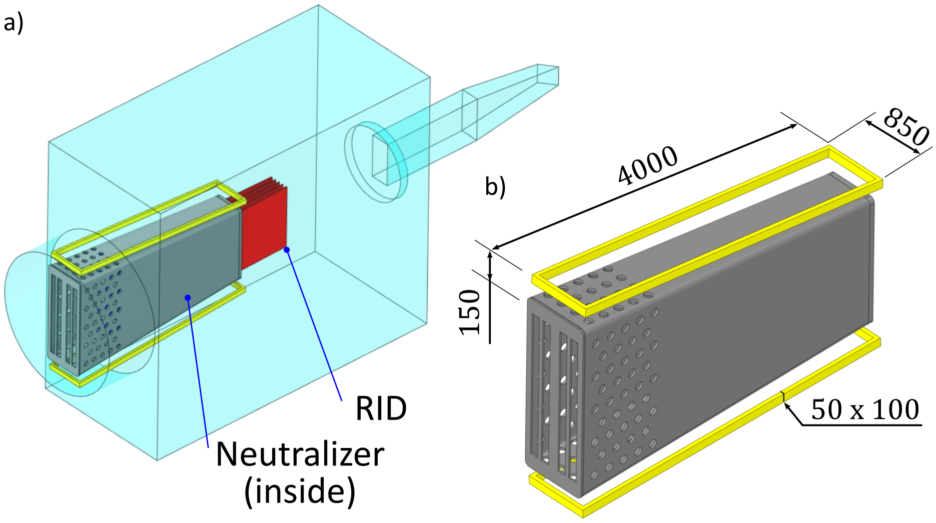

Figure 9. Case 3, a) View of the internal combined active and passive compensation applied to DTT; b) detail of the internal coil geometry.

SFSS design	$\eta_{\mathbf{stray}}$
External coils	0.925
Internal shield	0.961
Internal shield and coils	0.981

Table 2. Results summary for the considered SFSS designs.

stray field. The three design options for the SFSS, here fairly compared considering an integrated approach, represent an important basis for the choice and development of the SFSS for DTT NBI.

References

[1] R. Ambrosino, et al. *DTT - Divertor Tokamak Test facility: A testbed for DEMO*. Fus. Eng. Des. 167 (2021) 112330. DOI: 10.1016/j.fusengdes.2021.112330

[2] M. Hanada, et al. *Progress in development and design of the neutral beam injector for JT-60SA*. Fus. Eng. Des. 86 (2011) 835-838. DOI: 10.1016/j.fusengdes.2011.04.068

[3] S. Goetz, et al. *Design of Ion Removal System and Magnetic Shielding for the ASDEX-Upgrade Neutral Injection Beam Line.* Fusion Technology 1988, Vol. 1, 615-619.

[4] M. Roccella, et al. *Analysis of active and passive magnetic field reduction systems (MFRS) of the ITER NBI*. Fus. Eng. Des. 82 (2007) 709-715. DOI: 10.1016/j.fusengdes.2007.07.049

[5] G. Barrera, et al. *Magnetic analysis of the magnetic field reduction system of the ITER neutral beam injector*. Fus. Eng. Des. 96–97 (2015) 400-404. DOI: 10.1016/j.fusengdes.2015.02.054

[6] Molecular Flow User's Guide, pp. 62-78. COMSOL Multiphysics® v. 6.0. COMSOL AB, Stockholm, Sweden. 2021